PRZEGLĄD ELEKTROTECHNICZNY

1. Sergey GOOLAK[1], 2. Ievgen RIABOV[2], 3. Oleksandr GOROBCHENKO[1], 4. Viktor YURCHENKO[4],
5. Olena NEZLINA[1]

[1]State University of Infrastructure and Technologies, Faculty of Railway Rolling Stock Infrastructure, Department of Electromechanics and Rolling Stock Of Railways (1), Ukraine
[2] National Technical University «Kharkiv Polytechnic Institute», Institute of Education and Science in Power Motorering, Electronics and Electromechanics, Department of Electric Transport and Locomotive Motorering (2) Ukraine
ORCID: 1. 0000-0002-2294-5676; 2. 0000-0003-0753-514X; 3. 0000-0002-9868-3852; 4. . 0000-0002-5900-874X; 5. 0000-0003-1613-4057

Improvement of the model of an asynchronous traction motor of an electric locomotive by taking into account power losses

Abstract. В роботі запропоновано вдосконалену модель асинхронного тягового двигуна з врахуванням магнітних втрат в сталі двигуна, як функції часу, на основі рівнянь питомих втрат. При проведенні досліджень використана математична модель асинхронного двигуна, що виконана в програмному середовищі MATLab, За результатами моделювання отримано для номінального режиму роботи двигуна значення середніх магнітних втрат та часові діаграми магнітних втрат. Отримані результати порівнюються з паспортним даними двигуна.

Abstract. *The paper proposes an improved model of an asynchronous traction motor, taking into account magnetic losses in the steel of the motor, as a function of time, based on the equations of specific losses. When conducting research, a mathematical model of an asynchronous motor, made in the MATLab software environment, was used. Based on the simulation results, the value of average magnetic losses and time diagrams of magnetic losses were obtained for the nominal operating mode of the motor. The results obtained are compared with the passport data of the motor.*

Streszczenie. *W pracy zaproponowano udoskonalony model asynchronicznego silnika trakcyjnego uwzględniający straty magnetyczne w stali silnikowej w funkcji czasu, oparty na równaniach strat właściwych. W badaniach wykorzystano model matematyczny silnika indukcyjnego, wykonany w środowisku oprogramowania MATLab. Na podstawie wyników symulacji uzyskuje się wartości średnich strat magnetycznych oraz wykresy czasowe strat magnetycznych dla nominalnego trybu pracy silnika, a uzyskane wyniki porównuje się z danymi paszportowymi silnika.* (**Udoskonalenie modelu asynchronicznego silnika trakcyjnego lokomotywy elektrycznej poprzez uwzględnienie strat mocy**)

Keywords: асинхронний двигун, магнітні втрати, вихрові стуми, гістерезис.
Keywords: asynchronous motor, magnetic losses, vortex noises, hysteresis.
Słowa kluczowe: silnik indukcyjny, straty magnetyczne, prądy wirowe, histereza.

Introduction

When building a traction electric drive with asynchronous traction motors, their control systems are built as vector systems [4-6] and direct torque control systems [7-9]. In vector control systems, the spatial current vector of the motor stator, expressed in three-phase coordinates, is converted into a current vector, expressed in two-phase orthogonal coordinates. The two-phase stator current vector is decomposed into orthogonal components. Thus, two control channels are organized. One control channel regulates the flux linkage, the other – the rotation speed of the motor shaft. The flux linkage controller sets the current control signal along one of the coordinates, the speed controller – along the other. Speed controllers are proportional [4] or proportionally integral controllers [5,6]. After the flux linkage and speed controllers, the signals go to the current controllers, which set the value of the supply voltage of the asynchronous electric motor for each of the orthogonal coordinates. The flux linkage and current controllers are proportionally integral controllers [4-6]. They can also be organized based on the laws of fuzzy logic [10]. After that, the supply voltage reference signals depicted in orthogonal coordinates are converted into the supply voltage reference signals depicted in natural three-phase coordinates. Direct torque control systems are a special case of vector control systems. From the analysis of the

principles of operation of vector control systems, it follows that when modeling such systems, it is advisable to use the model of an induction motor in orthogonal coordinates.

In vector control systems, the two-phase moving coordinate system [4,6] and the two-phase fixed coordinate system oriented to the generalized voltage and current vectors [5] have received the greatest application. Accordingly, it would be advisable to perform the traction motor model either in a two-phase moving coordinate system [11-13], or in a two-phase stationary one, oriented to the generalized voltage and current vectors [14-16]. Despite the obvious advantages of such an approach to modeling a traction drive system associated with the ease of implementation of such models, a number of assumptions should be taken into account with this approach. The vector control models use the hypotheses that an asynchronous motor has symmetrical windings, and its power supply system is symmetrical [4-6]. In studies [17-19] it is shown that during operation in an asynchronous electric motor such defects as an interturn short circuit of the stator windings can occur. These defects lead to asymmetry of the traction motor stator windings and cause asymmetry of the stator system. In addition, during operation, the supports of semiconductor devices of the traction converter, which converts the voltage of the intermediate circuit into a system of three-phase voltages in

accordance with the voltages of the control system setting, deviate from the nominal values. Moreover, these resistance deviations can be carried out for each semiconductor device by a different value, which will lead to asymmetry in the supply voltages of the traction motor. This factor causes the asymmetry of the system of stator currents of the electric motor [20-22]. In addition, during the operation of electric rolling stock, the process of changing the voltage of the contact network is a non-deterministic process [23]. All these factors limit the use of models of vector control systems [4-6], which are based on the hypothesis of the symmetry of the power supply system and windings of the traction motor, since the models of an asynchronous motor in two-phase systems are not suitable for operation in asymmetric modes.

The solution to this problem can be modeling an asynchronous electric motor in natural three-phase coordinates with their subsequent transformation into the necessary two-phase ones. Such a mathematical model is given in the study [24]. The simulation model is made in the ORCID software environment. At the same time, the electrical part of the motor is made on electrical elements – supports and inductances. Replaceable inductances are made using controlled voltage sources. The magnetic and mechanical parts of the electric motor are implemented by means of structural elements. This approach to the implementation of the model of an asynchronous electric motor allows to correctly study its operation in conditions of asymmetric power supply. But the question of studying the operation of an electric motor under conditions of asymmetry of its windings remains open, since this model does not take into account the influence of asymmetry of the electric motor windings on the value of the inductance of the magnetization circuit.

The work [25] is devoted to the study of the operation of an asynchronous traction motor under conditions of asymmetry of the supply voltage system and asymmetry of the motor windings. The model of an asynchronous electric motor is based on the model given in [24]. But in the model [25], in contrast to the model [24], there is a block for taking into account the change in the inductance of the magnetization circuit when the geometric dimensions of the traction motor windings change, which makes it possible to study the operation of the electric motor with asymmetry of its windings.

Another important aspect in modeling an asynchronous electric motor is taking into account the saturation of its magnetic system, which affects the dynamic characteristics of the electric motor. There are at least two approaches to the compilation of mathematical models taking into account the saturation of the magnetic circuit of the circuit: the use of nonlinear coefficients in the equations [26-28] or the introduction of equations of fictitious electrical circuits into the model with linear coefficients [29-31]. The second method guarantees taking into account the change in the harmonic composition of voltages and currents through the saturation of the magnetic circuit, but requires a priori knowledge of the quantitative characteristics of the harmonic spectra, in addition, in practice, only a small number of harmonics can be taken into account here. That is why in most studies preference is given to the method with non-linear coefficients. The use of hysteresis-free magnetization curves in one form or another [32, 33] in order to take into account the nonlinear change in the inductance or mutual inductance due to saturation of the magnetic circle has become widespread in practical calculations. So, in the study [32], the saturation of the magnetic circuit of an asynchronous electric motor is taken into account by determining the inductance as a function of the current of the magnetization circuit. The inductance of the magnetization circle is determined in relative units by dividing the fluid by the nominal value. Then, by means of the obtained inductance value, the value of the electromagnetic torque is corrected. Studies [24,25] show that it is more correct to use the inductance as a function of the flux linkage of the magnetization circle.

Multiple computational experiments have found that the nature of the transitional process of starting an asynchronous motor on the model depends significantly on the value of the active resistance introduced into the magnetization circle. This resistance takes into account the losses in the magnetic circuit of the induction motor. The value of this resistance is one of the criteria for the adequacy of the computer model to a real induction motor. In addition, the value of active resistance in the magnetization circuit has a significant impact on the characteristics of an asynchronous motor in steady state. Taking into account the active resistance in the magnetization circuit according to the scheme of its series connection with the main inductance did not allow in some cases to obtain a sufficient correspondence between the parameters of the steady state mode on the model and the real ones [24]. Approximation to the real characteristics of the steady state results in a decrease in the active resistance of the magnetic circuit, or even a refusal to take this parameter into account. This leads to a distortion of transient processes, and also does not allow one to reliably take into account the loss models in the magnetic core. The way out of this contradiction was the approach when the model uses a parallel connection in the magnetization circuit of the phases of the main inductance and active resistance [24, 25].

An important factor in creating a model of an induction motor is to take into account magnetic losses in its magnetic circuit. A number of studies have been devoted to this problem [34–36]. In [34], an algorithm was proposed for determining an induction motor in a magnetic circuit based on empirical dependencies. Despite the obviously correct approach to solving the problem, a number of difficulties arise when implementing the proposed algorithm on a simulation model. These difficulties are connected with the difficulty of determining the parameters of the empirical dependence. The study [35] proposed a model for determining the losses in the magnetic circuit - losses in steel - as a function of the electromotive force (EMF) in the magnetic circuit and the frequencies of the higher harmonic components of the EMF. This approach will make it possible to take into account the non-linear nature of the magnetization curve of the magnetic material when determining losses in the steel of an induction motor. The proposed approach to the determination of losses in steel gives a good result in the steady state operation of the electric motor. During transients, it shows the worst results. This factor is caused by the need to determine the higher harmonic components of the EMF, that is, the application? implementation of the Fourier transform. Another approach to determining the losses in steel can be the approach given in the study [36], where it is proposed to determine the losses in the electric motor steel as a function of induction in the elements of the electric motor design and power frequency. This approach to determining losses in steel is relevant for a general industrial drive with an asynchronous motor. In such a drive, there is no frequent change in the operating mode of the electric motor and the process of changing the supply voltage is a deterministic process. In the case of a traction drive of an AC electric rolling stock, the process of changing the voltage is non-

deterministic and there is a frequent change in the operating mode of the traction electric drive.

In [37], for a pulsating current electric motor, an algorithm was proposed for determining magnetic losses in the motor steel as a function of the total magnetic flux and the motor shaft speed. The implementation of a mathematical model of a pulsating current traction motor, taking into account magnetic losses [38], and a comparison of the simulation results with the passport data of the prototype motor showed high simulation accuracy.

In this paper, the existing model of an asynchronous traction motor is supplemented with a block for accounting for losses in the steel of the electric motor. As a result of the simulation, the starting characteristics of the electric motor were obtained and comparisons of the obtained results with the passport data of the electric motor were made. When conducting research, a hypothesis is used about the deterministic nature of the change in the voltage of the contact network, the symmetrical and sinusoidal nature of the power supply system of the traction motor, and the invariable nature of the load on the motor shaft.

The article has the following structure: in the second section, the object of research is selected and the use of a mathematical model of an asynchronous electric motor is justified, which can operate with asymmetry and non-sinusoidal voltages of the power supply system. The third section presents a mathematical apparatus for determining magnetic losses in the steel of an asynchronous traction motor and implements its mathematical model in the MATLab software environment. On the simulation model, time diagrams of the moment, the rotational speed of the electric motor shaft, stator systems of currents and magnetic losses in the motor steel were obtained. For the steady state, average values of magnetic losses in the motor steel were obtained for the period. In the fourth section, comparisons of the obtained results with the passport data of the motor are made. At the end of the work there are conclusions.

Determination of the object of research and justification for the choice of a mathematical model of an asynchronous electric motor
Determination of the object of research

In the course of research, the determination of magnetic losses in steel and their influence on the starting characteristics of a traction asynchronous motor is carried out. When determining the object of research, it is advisable to choose the same type and power of a traction asynchronous motor, for which a number of studies have already been carried out, in particular, studies of its operation under conditions of asymmetry of its windings and asymmetry and non-sinusoidality of the power system. In the works [25,38], these studies were carried out for an asynchronous traction motor with a squirrel-cage rotor of the CTA1200 type with a power of 1200 kW. Therefore, it is logical to choose the indicated traction motor of the motor as an object of research.

Specifications of a traction asynchronous electric motor with a squirrel-cage rotor of the CTA1200 type are given in Table 1 [25].

Table 1. Technical characteristics of traction asynchronous electric motor with a squirrel-cage rotor of the CTA1200 type

Parameter	Value
Shaft power rating, P_{nom}, kW	1200
Rated phase voltage, U_{nom}, V	1079
Rated frequency of supply voltage, f_s, Hz	55,8
Rated rotation speed of a motor shaft in idle mode $n_{n.idle}$, rpm	1116
Nominal motor shaft speed n_n, rpm	1110

Rated torque on the motor shaft T_n, N·m	10417
Number of poles p	6
The number of turns of the stator winding w_s	48
The cross-sectional area of the stator back S_{sb}, m²	0,02816
The area of intersection of the stator teeth S_{st}, m²	0,07172
Stator back mass m_{sb}, kg	847
The mass of the stator teeth m_{st}, kg	177
Magnetic losses in the stator steel $P_{s.st}$, kW	13,6
Cross-sectional area of the rotor back S_{rb}, m²	0,03285
Cross-sectional area of rotor teeth S_{rt}, m²	0,06754
Mass of the back of the rotor m_{rb}, kg	305
Mass of rotor teeth m_{st}, kg	147
Magnetic losses in the steel of the rotor $P_{r.st}$, kW	2,3
Magnetic flux scattering coefficient, σ_Φ, %	4

Justification of the choice of a mathematical model of a traction asynchronous electric motor

In [25], an approach was applied to modeling an asynchronous motor powered by an asymmetric voltage system and can operate under conditions of asymmetry of its windings. In this model, the electrical part of the electric motor is detected by observing the electrical elements of the MATLab environment software, and the magnetic and mechanical parts are detected by observing the structural elements. In addition, the mutual inductance of the phases is carried out at looking controlled voltage sources. The key signals for these voltage sources are the respective mutual flux linkages of the phases. This allows to establish studies in the life of an asynchronous motor from an asymmetric and non-sinusoidal system of life voltages. In addition, in the data of the model there is a block that allows to set the dependence of the parameters of the electric motor on the geometric dimensions of its windings. Therefore, the model given in the study [25] was adopted as the basic mathematical model.

Development of a simulation model of a traction induction motor with rotation of magnetic losses in steel
The mathematical model shows the instantaneous values of magnetic losses in the electric motor steel

The work [37] analyzes the instantaneous value of the magnetic losses of the armature steel as a function of time during the oscillation period. The specific loss equation takes into account the accumulation of magnetic energy in steel. The representations can be used for any magnetic material and any geometry for which the material properties and magnetic flux subtleties are known. Specific power loss in electrical steel on vortex flows and hysteresis with rotation of accumulation of magnetic energy how it functions at magnetic penetration time μ μ_r =1 h/m, material volume V=1 m³ and material mass m=1 kg response to 1 kg levels

(1)
$$p_{loss}(t) = \left(H_c + K_{hyst} \cdot \left| B_p \cdot \sin(\omega t) \right| \right) \cdot \left| B_p \cdot \omega \cdot \cos(\omega t) \right| + K_{addy} \cdot B_p^2 \cdot \omega^2 \cdot \cos^2(\omega t),$$

where H_c – coercive force, A/(m·kg); B_p–induction amplitude, Tl; ω – magnetization reversal frequency, rad/s; t – time, s; K_{hyst} – coefficient taking into account specific hysteresis losses, m/(kg•H); K_{addy} – coefficient taking into account the specific eddy current losses, m/(kg·H·s); p_{loss}– specific power losses, W/(kg•m³).

Average losses in steel per unit volume [37]

(2)
$$\langle p_{loss}(t) \rangle = \left(\frac{2 \cdot H_c}{\pi} \cdot B_p + \frac{K_{hyst}}{\pi} \cdot B_p^2 \right) \cdot \omega + \frac{K_{addy}}{2} \cdot B_p^2 \cdot \omega^2.$$

The magnetization reversal frequency is found from the expression [37]

$$(3) \qquad \omega = \frac{2 \cdot \pi \cdot f}{p},$$

where p – the number of pairs of poles; f – magnetization reversal frequency, Hz. For the stator, f is equal to the frequency of the fundamental harmonic voltage f_1. For rotor

$$(4) \qquad f = f_1 \cdot s,$$

where s – motor slip.

$$(5) \qquad s = \frac{n_{idle} - n_{nom}}{n_{idle}},$$

where n_{nom} – nominal speed of the motor shaft, rpm; n_{idle} - motor shaft speed in idling mode, rpm.

$$(6) \qquad n_{idle} = \frac{f_1 \cdot 60}{p}.$$

The coefficients H_c, K_{hyst} i K_{addy} can be found from the passport data of electrical steel manufacturers using approximation.

Specific losses in electrical steel 2212 in accordance with the passport data are given in Table 2 [37].

Table 2. Passport data and data obtained as a result of the approximation of specific losses in electrical steel 2212

	B, T	0	0,5	0,6	0,7	0,8	0,9	1,0	1,1
f=50 Hz	p_{p50}, W/(kg·m³)	0	0,755	1,085	1,472	1,782	2,17	2,56	3,12
	p_{M50}, W/(kg·m³)	0	0,713	1,011	1,361	1,764	2,218	2,72	3,28
f=60 Hz	p_{p60}, W/(kg·m³)	0	0,953	1,335	1,811	2,192	2,669	3,15	3,83
	p_{M60}, W/(kg·m³)	0	0,877	1,244	1,675	2,169	2,728	3,35	4,04
	B, T	1,2	1,3	1,4	1,5	1,6	1,7	1,8	1,9
f=50 Hz	p_{p50}, W/(kg·m³)	3,798	4,573	5,348	6,123	6,975	7,673	8,53	9,69
	p_{M50}, W/(kg·m³)	3,892	4,554	5,268	6,034	6,852	7,722	8,64	9,62
f=60 Hz	p_{p60}, W/(kg·m³)	4,671	5,624	6,577	7,531	8,579	9,437	10,47	11,92
	p_{M60}, W/(kg·m³)	4,788	5,602	6,48	7,422	8,428	9,498	10,63	11,83

In the Table 2: f – frequency; p_{p50}, p_{M50}, p_{p50}, p_{M50} – respectively, the specific losses of electrical steel 2213 depending on the frequency (50 and 60 Hz) – passport data (p_{p50} and p_{p50}) and obtained by approximation (p_{M50} and p_{M60}).

For ease of approximation, expression (2) is presented as follows

$$(7) \quad p_{p50} = 4 \cdot H_c \cdot f \cdot B_p + \left(2 \cdot K_{hyst} \cdot f + 2 \cdot \pi^2 \cdot K_{addy} \cdot f^2\right) \cdot B_p^2,$$

Expression (7) is a function of induction and the square of induction. Let's apply the least squares approximation to it [37]. For this purpose, expression (4) is presented as follows

$$*8) \qquad p_{M50} = a \cdot B_p + b \cdot B_p^2,$$

where a and b – least squares approximation coefficients.

After performing the approximation, the values of the coefficients a=0,127 W/(kg·T·m³); b=2,597 W/(kg·T²·m³).

The values of specific losses at a reversal frequency of 50 Hz, obtained using the approximating function, are listed in Table 2.

To determine the unknown coefficients H_c, K_{hyst}, K_{addy} in equations (7) - (9), an additional equation was obtained by approximating the specific losses in steel at a reversal

frequency of 60 Hz. Calculations were made based on the following considerations. In [37], the specific losses for the reversal frequency 50 Hz and the induction amplitude of 1.0 T and for the reversal frequency 60 Hz and the induction amplitude of 1.5 T are given. The transition coefficient was calculated to determine the specific losses at a magnetization reversal frequency of 60 Hz, determined by the expression

$$(9) \qquad k_p = \frac{p_{1.5/60}}{p_{1.5/50}} = \frac{7,53}{6,123} = 1,23,$$

where $p_{1,5/50}$=6,123 W/(kg·m³) – specific losses at the magnetization reversal frequency of 50 Hz and induction amplitude of 1.5 Hz (Table 2).

Considering the foregoing, the specific losses at a magnetization reversal frequency of 60 Hz can be determined by the relation

$$(10) \qquad p_{p60} = k_p \cdot p_{p50}.$$

The results obtained are listed in Table 2, for which, similarly to expression (8), the least squares approximation was performed. After performing the approximation by the least squares method, the value of the coefficients a=0,16 W/(kg·T·m³); b=3,29 W/(kg·T²·m³).

The values of specific losses at a magnetization reversal frequency of 60 Hz, obtained using an approximating function, are listed in Table. 2.

According to the results of Table 2 plots the dependence of passport specific losses in electrical steel 2212 at frequencies of 50 Hz and 60 Hz (p_{p50} and p_{p6}, respectively) and their approximations (p_{M50} and p_{M60}, respectively) (Fig. 1).
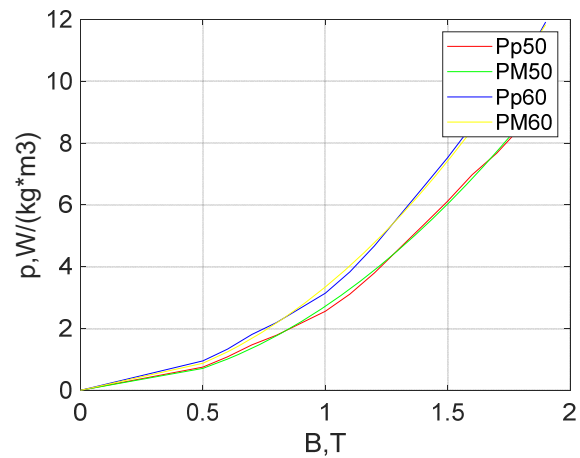

Fig.1. Specific losses of electrical steel: : p_{p50}, p_{p60} – passport data for a frequency of 50 and 60 Hz, respectively; p_{M50}, p_{M60} - results of approximation of specific losses in electrical steel for magnetization reversal frequencies of 50 and 60 Hz, respectively

The root-mean-square approximation error is determined, calculated in accordance with the expression

$$(11) \qquad \sigma_\delta = \frac{1}{N-1} \cdot \sqrt{\sum_{i=1}^{N} \left(\delta_{Mi} - \delta M_{mean}\right)^2},$$

where N – the number of approximation points; δ_{Mi} – approximation error at the i-th point; δ_{Mmean} – average value of the error.

The root-mean-square approximation error was 1.14%, which indicates a high degree of reliability of the results obtained.

From equations (7), (8), the expression for the coercive force for 50 (H_c) and 60 (H_{c1}) Hz was obtained:

(12)
$$\begin{cases} H_c = \dfrac{a}{4 \cdot f} = 0,000634 \dfrac{A}{kg \cdot m}; \\ H_{c1} = \dfrac{a_1}{4 \cdot f_1} = 0,00065, \dfrac{A}{kg \cdot m}, \end{cases}$$

where f=50 Hz; f_1=60 Hz; a=0,127 W/(kg·T·m³) – approximation coefficient (8) at a frequency of 50 Hz; a_1=0,16 W/(kg·T·m³) - approximation coefficient (5) at a frequency of 60 Hz.

To determine the coefficients K_{hyst} and K_{addy}, a system of equations is considered by comparing the coefficients for the variable $(B_p)^2$ in equations (7), (8).

(13)
$$\begin{cases} 2 \cdot K_{hyst} \cdot f + 2 \cdot \pi^2 \cdot K_{addy} \cdot f^2 = b, \\ 2 \cdot K_{hyst} \cdot f_1 + 2 \cdot \pi^2 \cdot K_{addy} \cdot f_1^2 = b_1, \end{cases}$$

where f = 50 Hz; f_1 = 60 Hz; b=2,597 W/(kg·T²·m³) – approximation coefficient (8) at a frequency of 50 Hz; b_1=3,29 W/(kg·T²·m³) - approximation coefficient (5) at a frequency of 60 Hz.

The values of the coefficients K_{hyst} and K_{addy} were obtained: K_{hyst}= 0,018 m/(kg·H) and K_{addy} = 1,449·10⁻⁷ m/(kg·H·s).

To implement the model of magnetic losses in electrical steel (1), (2), one should find the amplitudes of inductions in nodes made of electrical steel – the back and teeth of the armature [37].

The magnetic induction in the back of the stator is found by the expression

(14)
$$B_{sb} = \frac{\Phi_{\mu\Sigma m}}{2 \cdot S_{sb}}.$$

where S_{sb} – area of intersection of the stator back (Table 1); $\Phi_{\mu\Sigma m}$ – total magnetic flux of the motor magnetization circuit.

The magnetic induction in the stator teeth is found by the expression

(15)
$$B_t = \frac{\Phi_{s\Sigma m}}{S_t},$$

where S_t – area of intersection of the stator teeth (Table 1).

Since the magnetic induction in the stator and rotor teeth is non-sinusoidal, its value should be reduced to the value of the first harmonic by multiplying by the reduction factor. The coefficient of reduction to the first harmonic of the induction of the stator and rotor teeth is native π/2 [39]. Taking into account the reduction factor, expression (15) takes the form

(16)
$$B_z = \frac{\pi \cdot \Phi_{s\Sigma m}}{2 \cdot S_z}.$$

The total magnetic flux of the magnetization circuit was determined on a traction motor simulation model based on the following considerations. On the traction motor simulation model, it is possible to determine the flux linkage of the stator magnetization circuit separately for each phase of the electric motor. Magnetic for each phase was determined by the expression

(17)
$$\Phi_{si} = \frac{\Psi_{\mu i}}{k_w \cdot w_{si}},$$

where $\Psi_{\mu i}$ – flux linkage of the corresponding motor stator phase; w_{si} – the number of turns of the winding of the corresponding phase of the motor stator; k_w=0,925 – winding ratio.

Since the traction motor model is made in three-phase real coordinates, to determine the total modulus of the magnetic flux vector, one should first go to two-phase orthogonal coordinates.

The projections of the total magnetic flux vector on the axes of a two-phase orthogonal coordinate system have the form

(18)
$$\Phi_{sx} = \frac{2}{3} \cdot \left(\Phi_{s\alpha} + \Phi_{s\beta} \cdot cos\left(-\frac{2 \cdot \pi}{3} \right) + \Phi_{s\gamma} \cdot cos\left(\frac{2 \cdot \pi}{3} \right) \right);$$

(19)
$$\Phi_{sy} = \frac{2}{3} \cdot \left(\Phi_{s\alpha} + \Phi_{s\beta} \cdot sin\left(-\frac{2 \cdot \pi}{3} \right) + \Phi_{s\beta} \cdot sin\left(\frac{2 \cdot \pi}{3} \right) \right).$$

Then the total magnetic flux

(20)
$$\Phi_{s\Sigma m} = \sqrt{\Phi_{sx}^2 + \Phi_{sy}^2}.$$

The total magnetic losses of the motor stator steel are the sum of the magnetic losses in the back and stator teeth.

(21)
$$p_{sloss\Sigma}(t) = p_{sbloss}(t) + p_{stloss}(t),$$

where $P_{sbloss}(t)$, $P_{stloss}(t)$ – magnetic losses in the stator back and stator teeth, respectively.

Similarly, the average magnetic losses are calculated for the period

(22)
$$\langle P_{sloss\Sigma}(t) \rangle = \langle P_{sbloss}(t) \rangle + \langle P_{stloss}(t) \rangle,$$

where $<P_{sbloss}(t)>$, $<P_{stloss}(t)>$ – average magnetic losses in the stator back and stator teeth, respectively.

The reduced magnetic permeability of steel 2212 differs from 1 [37]. Moreover, it is an induction function [39]. The work [39] presents magnetization curves for electrical steel 2212 for the material from which the backs of the stator and rotor are made (Fig. 2) and the material from which the teeth of the stator and rotor are made (Fig. 3).
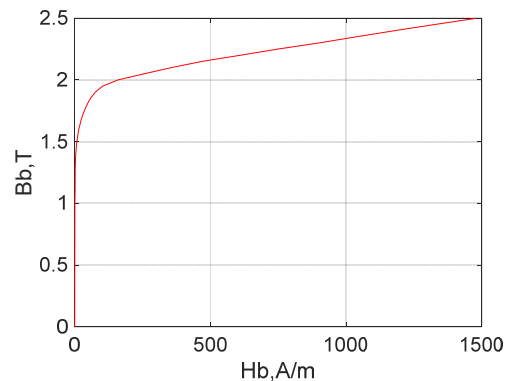

Fig. 2. The magnetization curve of electrical steel, from which the backs of the stator and rotor are made.

The magnetic permeability as a function of induction can be determined from the expression

(23)
$$B = \mu \cdot H,$$

where μ – magnetic permeability, H/m; B - induction, T; H - tension, A/m.

Then the magnetic permeability can be calculated using the formula
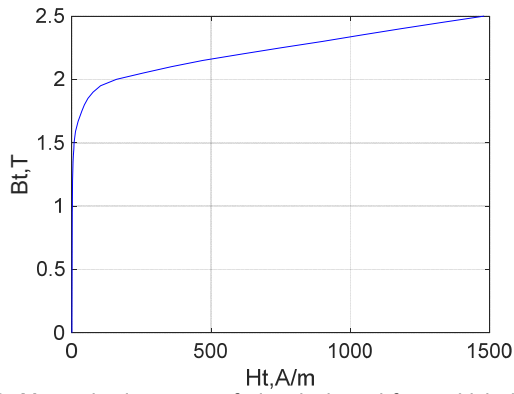
(24)
$$\mu = \frac{B}{H}.$$

Fig. 3. Magnetization curve of electrical steel from which the teeth of the stator and rotor are made

Based on the calculation results, graphs of the magnetic permeability of the backs of the stator and rotor and the teeth of the stator and rotor as functions of the corresponding inductions were plotted (Fig. 4).

Then the coefficients that take into account both hysteresis losses and eddy current losses have the form

$$(25) \qquad k_{hyst} = K_{hyst} \cdot \frac{\mu_r}{\mu_i},$$

$$(26) \qquad k_{addy} = K_{addy} \cdot \frac{\mu_r}{\mu_i},$$

where $\mu_r = 1$, H/m - magnetic permeability of the steel sample adopted in determining the specific losses of the generalized sheet of electrical steel; μ_i, H/m – magnetic permeability of the corresponding structural element.
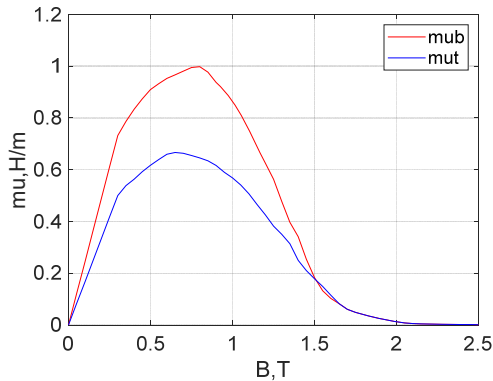

Fig.4. Dependence of magnetic permeability on induction: mub – stator and rotor backs; mut – stator and rotor teeth

The coefficients H_c, K_{hyst} and K_{addy} in equation (4) are determined for specific power losses expressed in W/(kg·m3). To convert to losses expressed in W, equations (1) and (2) are multiplied by the mass of steel of the corresponding structural element of the motor and its volume. The volume of a structural element is determined by the expression

$$(27) \qquad V_i = \frac{m_i}{\rho},$$

where m_i – mass of steel of the structural element, kg (Table 1); $\rho=7750$ kg/m^3 – specific gravity of electrical steel 2212.

The instantaneous values of losses in the back and stator teeth p, taking into account expressions (25-27), have the form:

$$(28) \qquad P_{sbloss}(t) = p_{sbloss}(t) \cdot \frac{m_{sb}^2}{\rho},$$

$$(29) \qquad P_{stloss}(t) = p_{stloss}(t) \cdot \frac{m_{st}^2}{\rho}.$$

Similarly, the average magnetic losses over the period in the steel of the back and stator teeth are found

$$(30) \qquad \langle P_{sbloss}(t) \rangle = \langle p_{sbloss}(t) \rangle \cdot \frac{m_{sb}^2}{\rho},$$

$$(31) \qquad \langle P_{stloss}(t) \rangle = \langle p_{stloss}(t) \rangle \cdot \frac{m_{st}^2}{\rho}.$$

Then the total instantaneous values of losses in the stator have the form

$$(32) \qquad P_{sloss}(t) = P_{sbloss}(t) + P_{stloss}(t).$$

Total average magnetic losses in the stator steel for the period

$$(33) \qquad \langle P_{sloss}(t) \rangle = \langle P_{sbloss}(t) \rangle + \langle P_{stloss}(t) \rangle.$$

The magnetic losses in the rotor were calculated in a similar way. But when calculating the magnetic losses in the rotor, the scattering of the magnetic flux was taken into account. Taking into account the scattering of the total magnetic flux, the magnetic flux of the rotor was determined by the formula

$$(34) \qquad \Phi_{r\Sigma m} = (1 - \sigma_\Phi) \cdot \Phi_{s\Sigma m},$$

where σ_Φ – magnetic flux leakage coefficient (Table 1).

Simulation model of an asynchronous traction motor, taking into account the instantaneous values of magnetic losses in the steel of the electric motor

Simulation model of an asynchronous traction motor, taking into account the instantaneous values of magnetic losses in the steel of the electric motor

The implementation of magnetic losses in the steel of the traction motor (Fig. 5) began with the determination of the stator magnetic flux of the traction motor, determined in accordance with expression (20). For this purpose, on the basis of expression (17), the magnetic fluxes of each phase of the stator were determined. After that, on the basis of expressions (18) and (19), the projections of the total flux of the magnetic stator on the axes of the two-phase orthogonal coordinate system were determined. The magnetic flux of the rotor was determined by expression (34). The implementation of the algorithm for determining the magnetic fluxes of the stator and rotor was combined into one unit – Unit for determining the magnetic flux.

The next step of the simulation modeling was the implementation of the calculation of inductions in the back and stator teeth in accordance with expressions (14), (16).

The elements for calculating inductions in the structural elements of the traction motor were combined into one block "The block for determining inductions in the structural elements of an asynchronous motor".

The implementation of losses in steel, changing in time based on equations (23), (24) and the implementation of average losses in steel over a period - equations (25), (26) are summarized in "The block for determining magnetic losses in steel of structural elements of an induction motor".
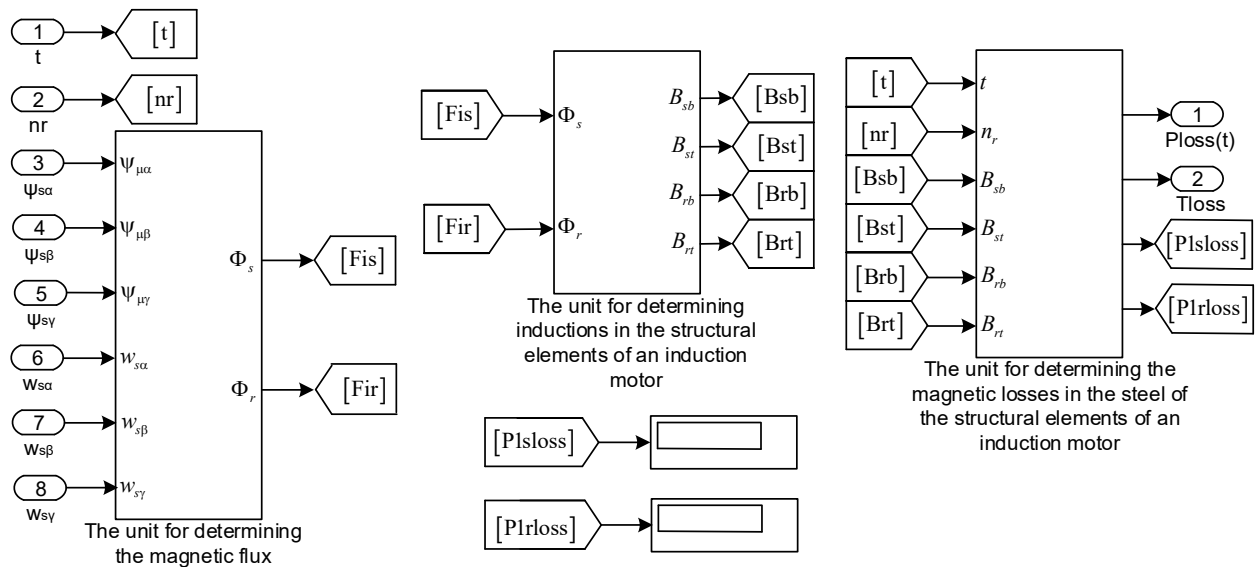
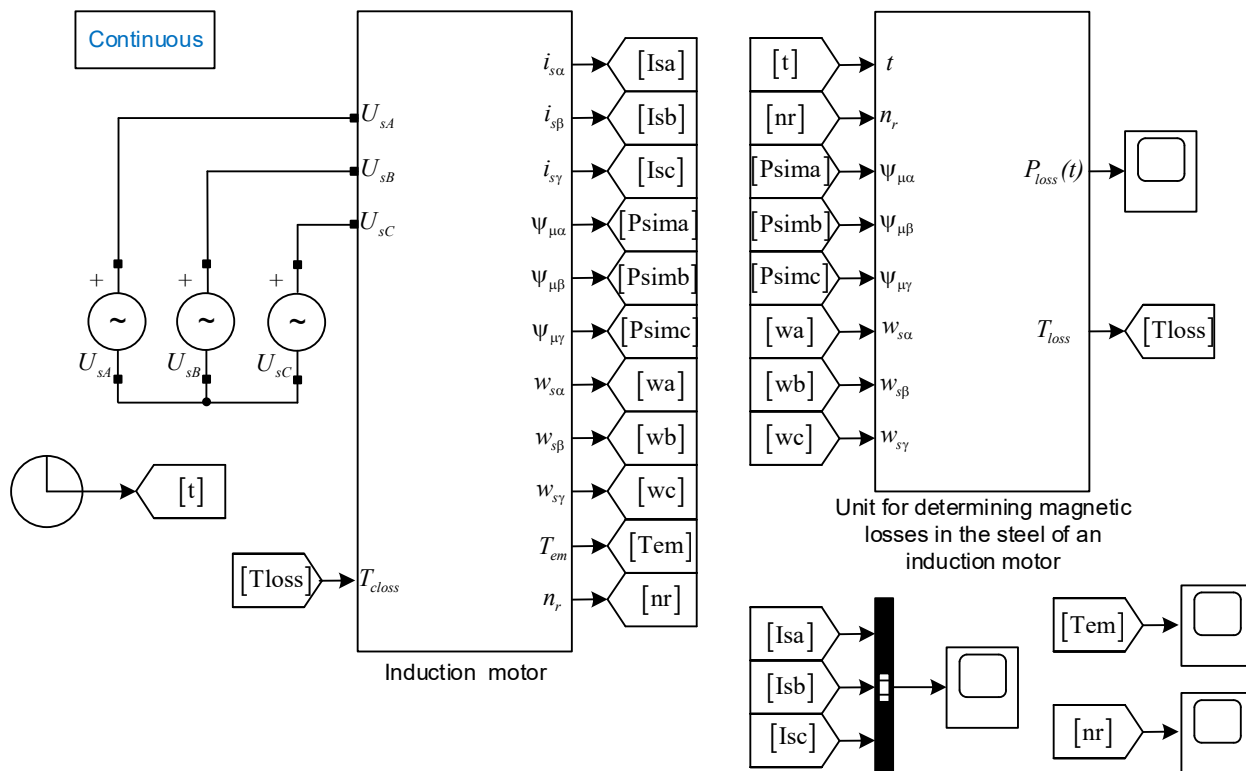Fig.5. Simulation model for determining magnetic losses in the steel of an induction motor

Fig.6. Simulation model of an asynchronous traction motor taking into account magnetic losses in the motor steel

The determinations of magnetic permeability in the back of the stator and rotor and the teeth of the stator and rotor are implemented in the form of tables using the elements of the 1-D Lookup Table of the Simulink library and are located in the Block for determining magnetic losses in steel of structural elements of an induction motor.

The simulation model for determining magnetic losses in the steel of an induction motor is combined into one block "Block for determining magnetic losses in the steel of an induction motor" (Fig. 6).

This block also includes a block for determining the total values of losses in the motor steel as the sum of instantaneous values of losses in the stator and rotor steel and a block for determining the static moment caused by magnetic losses in the steel. The static moment caused by magnetic losses in steel was determined using the formula.

$$(35) \qquad T_{closs}(t) = \frac{P_{loss}(t)}{\omega_{en}},$$

where $P_{loss}(t)$ - total instantaneous values of losses in the electric motor steel; ω_{en} – angular frequency of rotation of the motor shaft.

The induction motor model [25] is combined into one "Induction motor" block and supplemented with the "Tloss" input. In the "Induction motor" block, the total static moment is determined by the formula

$$(36) \qquad T_{c\Sigma}(t) = T_c + T_{closs}(t),$$

where Tc – static torque caused by the motor load.

A simulation model of an asynchronous traction motor, taking into account magnetic losses in the motor steel, is shown in Fig.6.

Simulation of the operation of an asynchronous traction motor, taking into account magnetic losses in the steel of the motor and analysis of the results
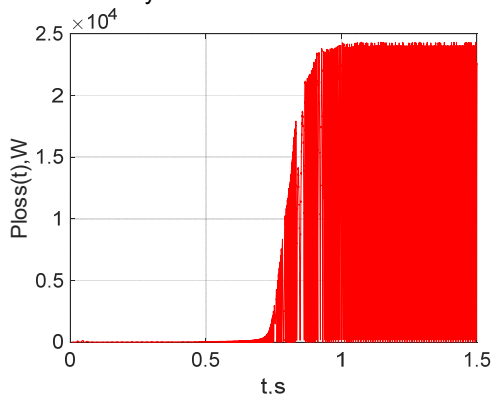

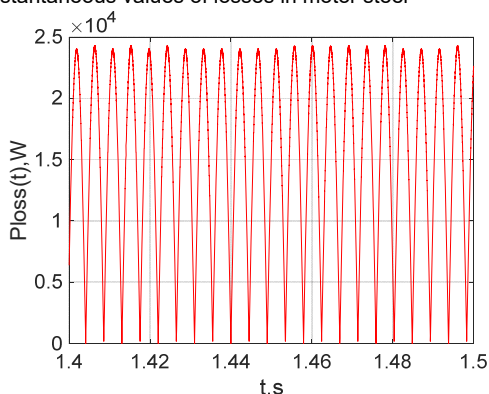Fig.7. Instantaneous values of losses in motor steel

Fig.8. Instantaneous values of losses in motor steel in steady state
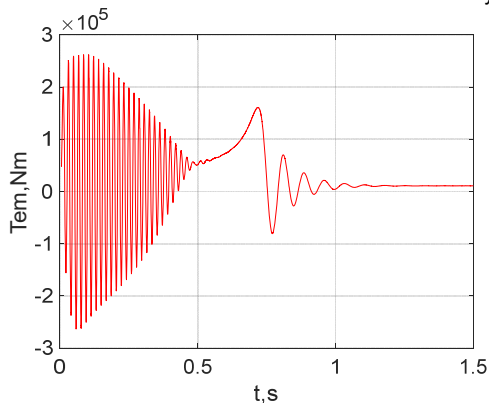

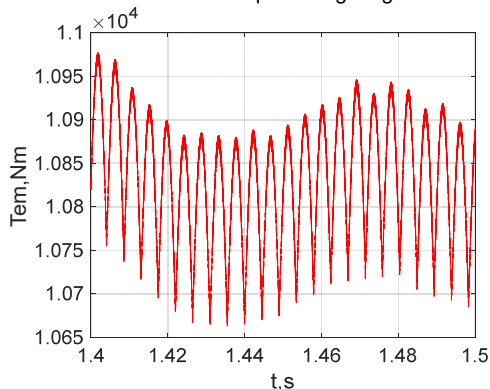Fig.9. Motor electromechanical torque timing diagram

Fig.10. Motor electromechanical torque timing diagram in steady state
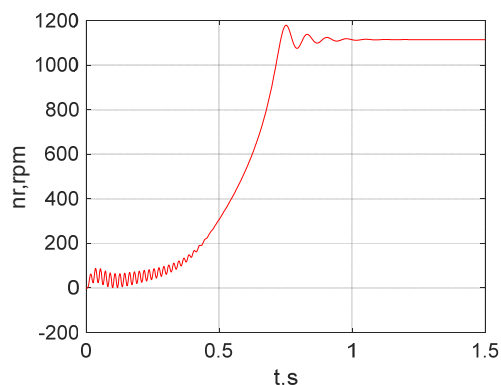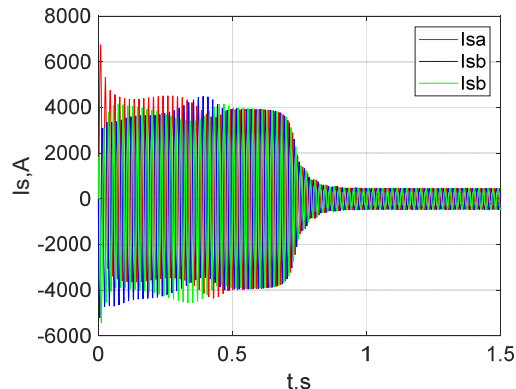

Fig.11. Motor speed timing diagram

Fig.12. Timing diagrams of motor stator currents

As a result of the simulation, the instantaneous values of losses in the motor steel (Fig. 7), the value of losses in the motor steel in steady state (Fig. 8), the electromechanical torque of the motor (Fig. 9), the electromechanical torque in steady state (Fig. 10), frequency of rotation of the motor shaft (Fig. 11) and stator currents (Fig. 12) were obtained.

In addition to the above diagrams, the simulation model obtained the values of magnetic losses in the steel of the stator and rotor, the frequency of rotation of the motor shaft in steady state, the electromechanical torque in steady state, and the amplitudes of the phase currents of the stator of the electric motor (Table 2).

Table 2. Comparison of simulation results with passport data of the traction motor

Parameter	Passport data	Model	Error σ, %
Amplitude of stator phase currents, A	450	451,7	0,4
Motor shaft speed, rpm	1110	1112,5	0,2
Torque, N·m	10417	10660	2,3
Magnetic losses in the stator steel, kW	13,6	13,11	3,6
Magnetic losses in the rotor steel, kW	2,3	2,284	0,7

The errors in determining the indicated parameters on the simulation model are calculated by the formula

$$(35) \qquad \sigma = \frac{A_{pd} - A_M}{A_{pd}} \cdot 100\%,$$

where A_{pd} – passport value of the quantity; A_M – value of the quantity obtained on the model.

Error values are listed in Table 2.

The analysis of the obtained results showed the following:
- the instantaneous value of magnetic losses in the steel of the motor changes according to a sinusoidal law with a

frequency that is twice the frequency of the supply of an asynchronous motor (Fig. 7, 8). This fact is important when calculating the power factor of the traction motor and the energy efficiency indicators of the traction motor as a whole;

- comparison of the simulation results with passport values of such quantities as the amplitude value of the stator phase currents, electromechanical torque, motor shaft speed, average values for the period of magnetic losses in the stator and rotor steel showed high accuracy of the simulation results. The errors in determining the values did not exceed 4%.

It follows from the analysis of the research results that the proposed simulation model of an asynchronous traction motor, taking into account magnetic losses in the motor steel, has high accuracy and can be used to study electrodynamic processes both in the asynchronous traction motor itself and to study electrodynamic processes in an asynchronous traction motor in general. Also, the proposed procedure for determining steel losses makes it possible to clarify the energy efficiency indicators of traction asynchronous electric motors and electric drives based on them, which are necessary to assess the technical performance of rolling stock [40].

Conclusaion

For research, a mathematical model of an asynchronous electric motor with a squirrel-cage rotor was chosen, which allows, without additional transformations of the model, to investigate the operation of an asynchronous electric motor in conditions of a poor-quality power supply system and asymmetry of its windings. The paper presents a method for calculating both instantaneous and average losses of magnetic losses in the motor steel over the period. A simulation model of an asynchronous traction motor has been developed taking into account magnetic losses in the steel of an asynchronous traction motor. Time diagrams of instantaneous values of magnetic losses in the motor steel, amplitude values of stator phase currents, electromechanical torque and rotational speed of the motor shaft are obtained. An analysis of the nature of the change in instantaneous losses in the steel of the electric motor showed that instantaneous losses change according to a sinusoidal law with a frequency twice the frequency of the supply of an asynchronous motor. Comparison of the simulation results with the passport data of the electric motor showed a high convergence of the simulation results. The error did not exceed 4%.

Authors: *PhD Sergey Goolak, State University of Infrastructure and Technologies, Department of Electromechanics and Rolling Stock of Railways, E-mail: sgoolak@gmail.com; PhD, Associate Professor Ievgen RIABOV, National Technical University «Kharkiv Polytechnic Institute», Department of Electric Transport and Locomotive Motorering (2), E-mail: riabov.ievgen@gmail.com; Prof. Oleksandr Gorobchenko, State University of Infrastructure and Technologies, Department of Electromechanics and Rolling Stock of Railways, E-mail: gorobchenko.a.n@gmail.com; Postgraduate Viktor Yurchenko, State University of Infrastructure and Technologies, Department of Electromechanics and Rolling Stock of Railways, E-mail: Vitekshef1997@gmail.com; PhD, Associate Professor Olena NEZLINA, State University of Infrastructure and Technologies, Department of Electromechanics and Rolling Stock of Railways,, E-mail: nezlina@ukr.net.*

REFERENCES
[1] Omelchenko, E., Tanich, V., Lymar, A. "Skidding Research of a Traction Asynchronous Electric Drive in the Electric Locomotive on a Dynamic Model", In *2021 International Ural Conference on Electrical Power Motorering (UralCon)*, pp. 513-518, IEEE, 2021.
[2] Titova, T. S., Evstaf'ev, A. M., Pugachev, A. A. "Improving the energy efficiency of electric drives for auxiliary units of traction rolling stock", In *Journal of Physics: Conference Series*, vol. 2131, no. 4, p. 042085, IOP Publishing, 2021.
[3] Wu, Z., Gao, C., Tang, T. "An Optimal Train Speed Profile Planning Method for Induction Motor Traction System", *Energies*, vol. 14, no 16, p. 5153, 2021.
[4] Kumar, Y.S., Poddar, G. "Medium-voltage vector control induction motor drive at zero frequency using modular multilevel converter", *IEEE Transactions on Industrial Electronics*, vol. 65 no 1, pp. 125-132, 2017.
[5] Hassan, M.M.; Shaikh, M.S.; Jadoon, H.U.K.; Atif, M.R.; Sardar, M. U. "Dynamic Modeling and Vector Control of AC Induction Traction Motor in China Railway", *Sukkur IBA Journal of Emerging Technologies*, *vol.* 3 no 2, pp. 115-125, 2020.
[6] Wang, H., Liu, Y.C., Ge, X. "Sliding-mode observer-based speed-sensorless vector control of linear induction motor with a parallel secondary resistance online identification", *IET Electric Power Applications*, *vol.* 12, no 8, pp. 1215-1224, 2018.
[7] Lee, J.K., Kim, J.W., Park, B.G. "Fast Anti-Slip Traction Control for Electric Vehicles Based on Direct Torque Control with Load Torque Observer of Traction Motor", In *2021 IEEE Transportation Electrification Conference & Expo (ITEC)*, pp. 321-326, IEEE, 2021.
[8] Aissa, B., Hamza, T., Yacine, G., Mohamed, N. "Impact of sensorless neural direct torque control in a fuel cell traction system", *International Journal of Electrical and Computer Motorering (IJECE)*, vol. 11, no 4, pp. 2725-2732, 2021.
[9] Karlovsky, P., Lettl, J. "Induction motor drive direct torque control and predictive torque control comparison based on switching pattern analysis", *Energies*, vol. 11, no 7, p. 1793, 2018.
[10]Butko, T., Babanin, A., Gorobchenko, A., "Rationale for the type of the membership function of fuzzy parameters of locomotive intelligent control systems", *Eastern-European Journal of Enterprise Technologies*, vol. 1, no 3, pp. 73, 2015.
[11]Li, W., Xu, Z., Zhang, Y. "Induction motor control system based on FOC algorithm", In *2019 IEEE 8th Joint International Information Technology and Artificial Intelligence Conference (ITAIC)*, pp. 1544-1548, IEEE, 2019.
[12]Liu, Z., Wu, J., Hao, L. "Coordinated and fault-tolerant control of tandem 15-phase induction motors in ship propulsion system", *IET Electric Power Applications*, vol. 12, no 1, pp. 91-97, 2018.
[13]Cherniy, S. P., Gudim, A. S., Buzikayeva, A. V. "Fuzzy multi-cascade AC drive control system", In *2018 International Multi-Conference on Industrial Motorering and Modern Technologies (FarEastCon)*, pp. 1-4, IEEE, 2018.
[14]Liao, Z., Zhao, Q., Zhang, X., Chen, L. "Research on Speed Sensorless Vector Control System of Asynchronous Motor Based on MRAS", In *MATEC Web of Conferences,* vol. 160, p. 02006, EDP Sciences, 2018.
[15]Yang, Z., Zhang, D., Sun, X., Ye, X. "Adaptive exponential sliding mode control for a bearingless induction motor based on a disturbance observer", *IEEE Access*, vol. 6, pp. 35425-35434, 2018.
[16]Im, N. K., Nguyen, V. S. "Artificial neural network controller for automatic ship berthing using head-up coordinate system", *International Journal of Naval Architecture and Ocean Motorering*, vol. 10, no 3, pp. 235-249, 2018.
[17]Kumar, P., Isha, T. B. "FEM based electromagnetic signature analysis of winding inter-turn short-circuit fault in inverter fed induction motor", *CES Transactions on Electrical Machines and Systems*, vol. 3, no 3, pp. 309-315, 2019.
[18]Goolak, S., Gerlici, J., Gubarevych, O., Lack, T., Pustovetov, M. "Imitation Modeling of an Inter-Turn Short Circuit of an Asynchronous Motor Stator Winding for Diagnostics of Auxiliary Electric Drives of Transport Infrastructure", *Communications - Scientific Letters of the University of Zilina*, vol. 23, no 2, pp. C65-C74, 2021.
[19]Gubarevych, O., Goolak, S., Daki, O., Tryshyn, V. "Investigation of Turn-To-Turn Closures of Stator Windings to Improve the Diagnostics System for Induction Motors", *Regional energy problems*, vol. 2, no 50, pp. 10-24, 2021.
[20]Fortes, M. Z., De Sousa, L. B., Quintanilha, G. M., Santana, C. E., de Oliveira Henriques, H. "Analysis of the Effects of Voltage Unbalance on Three-Phase Induction Motors", *International Journal of Energy and Sustainable Development*, vol. 3, no 2, pp. 29-37, 2018.

[21] Zhang, D., An, R., Wu, T. "Effect of voltage unbalance and distortion on the loss characteristics of three-phase cage induction motor", *IET Electric Power Applications*, vol. 12, no 2, pp. 264-270, 2018.

[22] Santos, V. S., Eras, J. J. C., Gutiérrez, A. S., Ulloa, M. J. C. "Assessment of the energy efficiency estimation methods on induction motors considering real-time monitoring", *Measurement*, vol. 136, pp. 237-247, 2019.

[23] Goolak, S., Tkachenko, V., Bureika, G., Vaičiūnas, G., "Method of spectral analysis of traction current of AC electric locomotives", *Transport*, vol. 35, no 6, pp. 658-668, 2020.

[24] Pustovetov, M. "Approach to implementation on a computer mathematical model of induction motor suitable for use as an integral part of models of electrotechnical complexes and systems", In *Modeling. Theory, methods and means*, pp. 332-345, 2016.

[25] Goolak, S., Liubarskyi, B., Sapronova, S., Tkachenko, V., Riabov, Ie., Glebova, M. "Improving a Model of the Induction Traction Motor Operation Involving Non-Symmetric Stator Windings", *Eastern-European Journal of Enterprise Technologies,* vol. 4, no 8(112), pp. 45–58, 2021.

[26] Syvokobylenko, V. F., Tkachenko, S. N. "The mathematical model of an induction machine in terms of the skin effect in the rotor and the saturation of magnetic circuits", In *2018 X International Conference on Electrical Power Drive Systems (ICEPDS)*, pp. 1-5, IEEE, 2018.

[27] Iegorov, O., Iegorova, O., Potryvaieva, N., Zaluzhna, H. "The Traction Induction Motor Magnetic Circuit Saturation Influence on the Variable Electric Drive Energy Efficiency", In *2021 IEEE International Conference on Modern Electrical and Energy Systems (MEES)*, pp. 1-5, IEEE, 2021.

[28] Zagirnyak, M., Chenchevoi, V., Ogar, V., Chencheva, O., Yatsiuk, R. "Refining induction machine characteristics at high saturation of steel", *Przeglad Elektrotechniczny*, vol. 96, no 11, pp. 119-123, 2020.

[29] Ghoggal, A., Hamida, A. H. "Transient and steady-state modelling of healthy and eccentric induction motors considering the main and third harmonic saturation factors", *IET Electric Power Applications*, vol. 13, no 7, pp. 901-913, 2019.

[30] Beleiu, H. G., Maier, V., Pavel, S. G., Birou, I., Pică, C. S., Dărab, P. C. "Harmonics consequences on drive systems with induction motor", *Applied Sciences*, vol. 10 no 4, pp. 1528, 2020.

[31] Xiao, X., Xu, W., Ge, J., Shangguan, Y. "Performance Analysis of Linear Induction Motors Considering Space and Time Harmonics", In *2021 13th International Symposium on Linear Drives for Industry Applications (LDIA)*, pp. 1-6, IEEE, 2021.

[32] Frolov, Y. M., Shelyakin, V. P., Sitnikov, N. V., Goremykin, S. A., Tonn, D. A. "Modeling an induction motor based on the equations of a generalized electric machine, taking into account the saturation of the magnetic circuit", In *E3S Web of Conferences*, vol. 178, p. 01011, EDP Sciences, 2020.

[33] Choi, S.-B., Wereley, N.M., Li, W. "Controllable Electrorheological and Magnetorheological Materials", *Frontiers Media SA: Laussane, Switzerland*, 164 p., 2019.

[34] Zagirnyak, M., Prus, V., Rodkin, D., Zachepa, Y., Chenchevoi, V. "A refined method for the calculation of steel losses at alternating current", *Archives of electrical motorering*, vol. 68 no 2, pp. 295—308, 2019.

[35] Zagirnyak, M., Ogar, V., Chenchevoi, V., Yatsiuk, R. (2022), "The determination of induction motor losses in steel taking into account its saturation", *COMPEL - The international journal for computation and mathematics in electrical and electronic motorering*, vol. ahead-of-print no. ahead-of-print.

[36] B. A. Nasir. "An accurate iron core loss model in the equivalent circuit of induction machines", *Journal Of Energy, Hindawi Publisher*, vol. 2020, pp 1-10, 2020.

[37] Goolak, S., Sapronova, S., Tkachenko, V., Riabov, Ie., Batrak, Ye. "Improvement of the Model of Power Losses in the Pulsed Current Traction Motor in an Electric Locomotive", *Eastern-European Journal of Enterprise Technologies*, vol. 6, no 5 (108), pp. 38–46, 2020.

[38] Goolak, S., Riabov, I., Tkachenko, V., Sapronova, S., Rubanik, I. "Model of pulsating current traction motor taking into consideration magnetic losses in steel", *Electrical Motorering & Electromechanics*, vol. 6, pp. 11–17, 2021.

[39] Kopylov, I.P. "Design of electrical machines", *Urayt publishing house*, 276 p., 2018.

[40] Kuznetsov, V., Kardas-Cinal, E., Gołębiowski, P., Liubarskyi, B., Gasanov, M., Riabov, I., Kondratieva, L., Opala, M. "Method of Selecting Energy-Efficient Parameters of an Electric Asynchronous Traction Motor for Diesel Shunting Locomotives—Case Study on the Example of a Locomotive Series ChME3 (ЧМЭ3, ČME3, ČKD S200)", *Energies,* vol. 15, pp. 317, 2022.